HHS Public Access

Author manuscript

Bone. Author manuscript; available in PMC 2017 December 01.

Published in final edited form as:

Bone. 2016 December ; 93: 79–85. doi:10.1016/j.bone.2016.09.013.

Single Dose of Bisphosphonate Preserves Gains in Bone Mass Following Cessation of Sclerostin Antibody in Brtl/+ Osteogenesis Imperfecta Model

Joseph E. Perosky[1], **Basma M. Khoury**[1], **Terese N. Jenks**[1,2], **Ferrous S. Ward**[1,2], **Kai Cortright**[1,2], **Bethany Meyer**[1,2], **David K. Barton**[1,2], **Benjamin P. Sinder**[1,2], **Joan C. Marini**[3], **Michelle S. Caird**[1], and **Kenneth M. Kozloff**[1,2,*]

[1]University of Michigan Department of Orthopaedic Surgery, Ann Arbor, MI

[2]University of Michigan Department of Biomedical Engineering, Ann Arbor, MI

[3]Bone and Extracellular Matrix Branch, National Institute of Child Health and Human Disorders, NIH, Bethesda MD

Abstract

Sclerostin antibody has demonstrated a bone-forming effect in pre-clinical models of osteogenesis imperfecta, where mutations in collagen or collagen-associated proteins often result in high bone fragility in pediatric patients. Cessation studies in osteoporotic patients have demonstrated that sclerostin antibody, like intermittent PTH treatment, requires sequential anti-resorptive therapy to preserve the anabolic effects in adult populations. However, the persistence of anabolic gains from either drug has not been explored clinically in OI, or in any animal model. To determine whether cessation of sclerostin antibody therapy in a growing OI skeleton requires sequential anti-resorptive treatment to preserve anabolic gains in bone mass, we treated 3 week old Brtl/+ and wild type mice for 5 weeks with SclAb, and then withdrew treatment for an additional 6 weeks. Trabecular bone loss was evident following cessation, but was preserved in a dose-dependent manner with single administration of pamidronate at the time of cessation. In vivo longitudinal near-infrared optical imaging of cathepsin K activation in the proximal tibia suggests an anti-resorptive effect of both SclAb and pamidronate which is reversed after three weeks of cessation. Cortical bone was considerably less susceptible to cessation effects, and showed no structural or functional deficits in the absence of pamidronate during this cessation period. In conclusion, while SclAb induces a considerable anabolic gain in the rapidly growing Brtl/+ murine model of OI, a single sequential dose of antiresorptive drug is required to maintain bone mass at trabecular sites for 6 weeks following cessation.

[*]Corresponding Author: 2015 Biomedical Science Research Building, 109 Zina Pitcher Place, Ann Arbor, MI 48109, kenkoz@umich.edu.

Keywords

Osteogenesis Imperfecta; Sclerostin Antibody; Cessation; Bisphosphonate; Osteoporosis

1. Introduction

Osteogenesis Imperfecta (OI) is a genetic disorder resulting from mutations in type I collagen or collagen-related proteins [1]. The OI phenotype is characterized by low bone mineral density (BMD), high turnover, high bone fragility, and has major manifestations during growth and development [2]. Current clinical treatment strategies for OI have focused on resolving the low bone mass characteristic of the disease through pharmacologic therapies. Anti-resorptive bisphosphonates are the most commonly used pharmacologic treatment for OI. Recent reviews and meta-analyses have shown that bisphosphonates can increase bone mineral density, particularly at metaphyseal sites, but do not induce significant reductions in fracture rates, particularly in the appendicular skeleton [3, 4]. Bisphosphonate treatment of OI mouse models recapitulate many of these clinical observations, and have not shown strong gains in cortical bone mass at long bone sites [5–8]. Furthermore, concern for long-term anti-resorptive consequences in the pediatric OI skeleton [9–13] suggest prudence in minimizing antiresorptive intervention while exploring alternate approaches to increase bone mass in OI. Recent studies suggest potential for intermittent parathyroid hormone (PTH) to improve bone mass in some mild adult OI patients, but such use is contraindicated for pediatric applications [14, 15].

Sclerostin antibody (SclAb) therapy represents an emerging anabolic strategy to treat OI patients for their low bone mass and high fracture susceptibility [16–21]. Sclerostin is secreted primarily by osteocytes and inhibits canonical Wnt signaling by binding to LRP4/5/6 on osteoblast lineage cells (MSCs, pre-osteoblasts, osteoblasts, lining cells, osteocytes) to inhibit bone formation [22]. Antibodies to sclerostin can reduce this inhibitory signal allowing Wnt signaling to proceed and resulting in upregulation of osteoblast activity and new bone formation [23]. Furthermore, a reduction in osteoclast activity has been noted with treatment [24, 25], suggesting a decoupling of bone formation and resorption in a manner that is consistent with promoting increased bone mass. Antibodies to sclerostin have shown a positive effect in pre-clinical [23, 24, 26, 27] and clinical studies [28–31] of osteoporosis, suggesting that this course of treatment may be beneficial for other diseases of low bone mass such as OI.

Previously, we have demonstrated a positive anabolic effect of SclAb treatment in young [19, 32], adolescent [18], and mature [20] Brtl/+ mice. Brtl/+ mice are heterozygous for a glycine to cysteine substitution (Gly349Cys) in *col1a1*, replicating many phenotypic features of Type IV OI [33–35]. When treated between 3 and 8 weeks of age with SclAb, young Brtl/+ mice showed anabolic gains in distal femoral metaphyseal bone, and cortical thickening through conversion of resorptive surfaces to formation surfaces [19]. These changes in architecture were enough to significantly increase the mechanical properties of the femur, despite continued synthesis of mutant collagen protein in bone.

Given that OI therapies are often administered during periods of rapid growth, an important consideration for the therapeutic use of SclAb is whether the anabolic effects are sustained following treatment cessation. In osteoporosis, adults treated with PTH, the only clinically available anabolic agent, demonstrate a time-dependent recovery in remodeling indices following PTH cessation, requiring subsequent BP to protect gains in bone mass [36, 37]. Clinical studies suggest that SclAb similarly results in gradual loss of bone mass gains after withdrawal in osteoporotic patients [38], supporting a similar need for follow-on administration of an anti-resorptive agent. While PTH has been studied in adults with OI, there is no data in the literature describing cessation effects of anabolic bone drugs such as PTH or SclAb in OI patients—adults or children [14, 15]—or in any mouse model of the disease [16–21]. In the present study, we hypothesize that cessation of SclAb would result in a gradual return of the OI fragility phenotype, which could be prevented by a single dose of bisphosphonate at the start of the SclAb cessation period.

2. Materials and Methods

2.1 Experimental Design

Three week old male Brtl/+ and WT mice were randomly assigned to control and cessation cohorts. Control mice (n=10–11/group) were used to establish the baseline phenotype of mice following 5 weeks of SclAb (25 mg/kg, twice per week [19]; SclAb VI, Amgen, Thousand Oaks, CA) or saline (PBS). Mice were then euthanized at 8 weeks of age. Mice from the cessation cohort were similarly treated with SclAb between 3 and 8 weeks of age. These mice were subsequently randomly divided into one of three cessation groups (n=10–11/group) where a single injection of PBS, low dose pamidronate (1.25 mg/kg), or high dose pamidronate (2.5 mg/kg) was given at 8 weeks of age. Pamidronate doses were chosen based on prior doses that preserved bone mass following PTH cessation [39]. No additional treatment was provided during the 6 week cessation period. These mice were then euthanized at 14 weeks of age by CO2 inhalation. Femora and L5 vertebrae were dissected free of soft tissue, wrapped in saline-soaked gauze, and frozen at −20°C until testing. Animals were housed in specific pathogen free cages with standard 12 hour light/dark cycles, and ad lib access to food water. All studies were approved by the University of Michigan Committee on Use and Care of Animals.

2.2 In Vivo Near-Infrared Optical Imaging

A non-invasive molecular imaging approach was undertaken to monitor bone turnover following cessation of SclAb using two separate imaging strategies [40, 41]. At 8 weeks of age, mice in the cessation cohort were administered a single injection of a near-infrared tetracycline (IRDye 800CW BoneTag, 80 nmole/kg i.v., LI-COR Biosciences, Lincoln NE) to label newly formed bone at the growth plate. A similar strategy was previously employed to monitor bone loss in the presence or absence of protective bisphosphonate therapy [41]. As a surrogate marker for osteoclast activity, mice were also administered a cathepsin K-activatable fluorescence imaging probe (CatK680 FAST, Perkin Elmer) at 8 weeks. This technique was previously used to monitor upregulation of osteoclast activity prior to observation of bone loss by microCT imaging following ovariectomy [40]. 24 hours after injection, mice were imaged by near-infrared fluorescence reflectance imaging (Pearl

Impulse, LI-COR Biosciences) to quantify baseline tetracycline binding and bone resorption at the proximal tibial growth plate. Sequential injections of CatK680 FAST at 11 and 14 weeks were followed by fluorescence imaging to monitor osteoclast activity during the entire cessation period. Percent retention of tetracycline was quantified at these time points as well by comparing 11 and 14 week proximal tibial fluorescence to 8 week values. All NIR analysis for both Cathepsin K and tetracycline was performed at the proximal tibia to minimize photon absorption through soft tissue and maximize signal-to-noise levels.

2.3 Ex Vivo Micro-computed Tomography

Femora and L5 vertebrae were imaged by micro-computed tomography (microCT) (eXplore Locus SP, GE Healthcare Pre-Clinical Imaging, London, ON, Canada). Specimens were immersed in water and scanned four at a time using the Parker method (180 degrees plus a 20 degree fan angle) at 80 kVp and 80μA with added filtration in the form of both an acrylic beam flattener and a 0.02 inch aluminum filter. Images were reconstructed at 18 μm voxel size, calibrated for densitometry, and rotated into a standard vertical position aligning the anterior-posterior axis of the bone with the x-axis of the scan, using the distal femoral condyles as an anatomic landmark [42]. Femoral cortical regions of interest spanning 15% total femoral length were centered midway between the lateral third trochanter and the distal femoral growth plate. Regions were segmented using a threshold of 2000 Hounsfield units, and cortical area, marrow area, and bending moment of inertia about the medial-lateral axis (Iyy) were measured.

Femoral trabecular regions of interest were isolated proximal to the distal femoral growth plate spanning 10% of the overall femoral length. The entire vertebral trabecular volume was isolated using a splining algorithm and manual contouring. Trabecular bone from both bones was subject to a specimen specific local autothreshold as previously described [43]. All analysis was performed using commercially available software (MicroView v2.2. Advanced Bone Analysis Application, GE Healthcare Pre-Clinical Imaging, London, ON).

2.4 Mechanical Testing

Femora were loaded to failure in four-point bending at 0.5 mm/s in the anterior-posterior direction using a servohydraulic testing machine (858 Minibionix II; MTS Systems Corporation, Eden Prairie, MN, USA) with the posterior side in tension between upper and lower supports that were 2.2 mm and 6.35 mm apart, respectively. Vertebrae were loaded to failure in uniaxial monotonic compression at 0.05 mm/s using the same apparatus with a custom-built fixture as previously described [44]. All bones were tested at room temperature and kept hydrated with PBS. Crosshead displacement was recorded by using an external linear variable differential transducer (LVDT; Lucas Schavitts, Hampton, VA, USA), and load data were collected with a 50-lb load cell (Sensotec, Columbus, OH, USA) at a sampling frequency of 2048 Hz. Load-displacement curves were analyzed for whole bone stiffness, yield load, ultimate load, and total energy (ultimate) to failure using a custom script (MATLAB 7.11; Mathworks Inc., Natick, MA, USA).

2.5 Data Analysis

MicroCT and mechanical testing data were assessed by mixed model, one-way ANOVA followed by Bonferroni post-hoc tests. In case of longitudinal paired *in vivo* data assessing Bonetag and CatK fluorescence imaging, a within-sample repeated measures ANOVA was used. Results are presented as mean ± standard deviation. All data was analyzed using IBM SPSS Statistics V.21 (SPSS, Inc., Chicago, IL, USA). $p<0.05$ was considered statistically significant unless stated otherwise.

3. Results

3.1 Retention of trabecular anabolic gains requires sequential antiresorptive treatment

Five weeks of SclAb treatment leads to significant gains in distal femoral BV/TV in both Brtl/+ (42%) and WT (49%) (Fig 1A). 6 weeks of untreated (PBS) cessation resulted in significant reductions in BV/TV in both Brtl/+ (−50%) and WT (−43%) compared to precessation levels (Fig. 1A). In Brtl/+, this was dominantly realized through a 44% reduction in trabecular number (Fig. 1B), while WT showed 18% reduction in trabecular thickness vs. 8 week values (Fig. 1C). A single injection of pamidronate achieved a dose-dependent preservation of the anabolic gains, almost entirely through preservation of trabecular number in both Brtl/+ and WT. These changes in Brtl/+ distal femoral trabecular bone volume are represented in images at baseline (Fig. 1D) and following cessation (Fig. 1E). MicroCT analysis of trabecular regions of L5 vertebrae yielded similar results to those of the femoral long bones. SclAb induced significant increases in trabecular number (Brtl/+ 18%; WT 15%) and thickness (Brtl/+ 38%; WT 57%) after 5 weeks of treatment leading to overall improvements in lumbar spine bone volume fraction (Brtl/+ 65%; WT 78%), compressive ultimate load (Brtl/+ 65%; WT 120%), and compressive energy (Brtl/+ 150%; WT 131%) (Fig. 2). Following 6 weeks of cessation from SclAb, trabecular number, thickness, and volume fraction all were lower in both Brtl/+ and WT vs. post-treatment values. In WT, these changes translated to a significantly lower compressive ultimate load. Single pamidronate administration upon SclAb cessation led to dose-dependent preservation of trabecular number, but was insufficient to fully preserve thickness and volume fraction in both Brtl/+ and WT (Fig. 2). Brtl/+ showed no change in biomechanical properties after cessation, while WT was rescued from cessation-induced reductions in ultimate load with increasing doses of pamidronate.

3.2 Femoral cortical bone structure and mechanics are retained following SclAb cessation

SclAb lead to significant improvements in femoral diaphyseal cortical area (Brtl/+ 30%; WT 54%), leading to functional improvements in yield load, ultimate load, and bending stiffness (Fig. 3). Following cessation of SclAb treatment, anabolic gains that had occurred in Brtl/+ over the prior 5 week treatment interval were sustained, with no significant differences in cortical area or bending moment of inertia between any of the groups (Fig. 3). No significant changes in yield load, ultimate load, stiffness, plastic energy, or post-yield displacement were observed by four-point bending following cessation of SclAb in Brtl/+. WT mice showed a significantly lower cortical area and anterior-posterior bending moment (Iyy) upon SclAb cessation, leading to reduced ultimate load. However, these values remained greater than untreated controls at 8 weeks of age.

3.3 In vivo imaging reveals restoration of osteoclast activity

Loss of proximal tibial trabecular bone labeled at 8 weeks was confirmed through longitudinal imaging of near-infrared tetracycline deposited at the time of SclAb cessation. Progressive loss of tetracycline signal in untreated mice was partially prevented with increasing doses of pamidronate (Fig. 4). In vivo cathepsin K imaging reveals a decrease in cathepsin K activity between 8 and 11 weeks in all groups, followed by an apparent rebound of bone resorption after an additional 3 weeks of SclAb cessation (Fig. 5).

4. Discussion

We have previously demonstrated that five weeks of SclAb therapy during periods of rapid bone growth induces significant anabolic gains in the Brtl/+ mouse model of type IV OI [19]. In the present study, we verify these observations and extend our outcomes to the dynamics of trabecular and cortical bone turnover following cessation of SclAb. In the 6 week cessation period, Brtl/+ cortical bone mass and biomechanical properties were not susceptible to cessation-induced changes, and remained at 8 week treated levels following the 6 weeks of cessation, independent of bisphosphonate administration. Conversely, WT and Brtl/+ mice were not able to sustain anabolic gains at trabecular bone sites, including the distal femur and lumbar vertebrae without inclusion of bisphosphonate treatment upon cessation.

There is precedent for anabolic osteoporosis therapies requiring antiresorptive treatment upon cessation to preserve anabolic gains in bone mass. Post-menopausal osteoporotic women required continuous alendronate therapy to preserve bone mineral density in the spine following 1 year of PTH (1-84) [36]. Similarly, despite large BMD gains during 1 year of blosozumab anti-sclerostin treatment, anabolic gains were not fully sustained in the year following blosozumab cessation [38]. Our current study extends these observations to a pediatric model of OI, where low bone mass and quality contribute to a need for anabolic stimulus during growth to improve resistance to fracture.

Clinically, in post-menopausal women with low bone mineral density, sclerostin antibodies induce a rapid increase in biochemical markers for bone formation that gradually return to baseline levels over the course of 1 year of treatment [28, 31]. Rapid decreases in resorption markers are also evident, but are more modest and variable [28, 31]. In the year following cessation of sclerostin antibody, a moderate increase in serum CTX corresponded with drug clearance and gradual return of bone mass toward pre-treatment levels [38]. These findings suggest an upregulation of bone resorption following SclAb cessation.

To gain insight into the trabecular bone loss following SclAb cessation in Brtl/+, we used longitudinal near-infrared optical imaging tools to quantify bone loss and osteoclast activity in the proximal tibia. In vivo imaging of molecular probes sensitive to cathepsin K-cleavage has previously been shown to demonstrate site-specific upregulation of osteoclast activity in mice following ovariectomy [40]. Here, we used a similar approach to monitor bone turnover in animals after cessation of SclAb. Over the first three weeks of cessation, Brtl/+ mice showed 10–20% decrease in cathepsin K-sensitive fluorescence, with an indication toward a dose-response with increasing pamidronate given at 8 weeks. We have previously

indicated a modest anti-resorptive effect of SclAb through serum biomarkers and histomorphometric analysis in 8 week [19], 10 week [18], and 6 month Brtl/+ mice [20]. Aged rats subject to ovariectomy for 8 weeks and treated with SclAb showed a dose-dependent suppression of lumbar vertebral osteoclast surface that was removed upon cessation of drug [25]. As a result, trabecular bone volume fraction increased dose-dependently during the treatment period, but gains were reversed following cessation. Changes in expression of osteoclast-related genes indicated an increase of the RANKL/OPG ratio in osteoblasts following 18 weeks of cessation [25]. Findings in the current study may suggest a prolonged antiresorptive effect from 8 to 11 weeks followed by osteoclast rebound as the drug is cleared, resulting in the observed reductions in trabecular bone by 14 weeks of age. Bone turnover activity in the proximal tibia was further confirmed by monitoring loss of a near-infrared tetracycline administered at the time cessation. Here, deposition of BoneTag 800 at 8 weeks was visualized, and progressive loss of signal was observed between 3–6 weeks of cessation, with more retention evident in pamidronate treated bone. Although the relative magnitude of bone loss vs. fluorescent signal loss differed between NIR imaging and microCT, these differences are explained due to the tetracycline only incorporating in a focal region of newly forming bone near the proximal tibial growth plate rather than the full trabecular region of interest measured by microCT in the distal femur.

In contrast to the trabecular data, femoral cortical bone mass and strength remained at SclAb treatment levels following cessation in Brtl/+, with sustained treatment values of bending load and stiffness. Clinically, 1 year of blosozumab cessation resulted in more severe loss of BMD in the lumbar spine, while total hip and femoral neck BMD showed a more gradual reduction following cessation [38]. Together, these data suggest that in both young and aged skeletons, the cortical compartment appears to be less susceptible to cessation-induced loss of anabolic gains, however longer-term studies may indicate a more gradual return of the cortical fragility phenotype.

Current clinical treatment strategies for OI involve continuous bisphosphonate treatment through skeletal maturity. In the present study, we treated mice with a classic OI-causing mutation with anabolic SclAb during periods of rapid bone growth through a period in which body mass increases plateau [19]. Single-dose bisphosphonate therapy was sufficient to maintain trabecular bone mass for a period of time surpassing the treatment duration. Repeated dosing intervals will likely be necessary, as indicated by NIR imaging which suggests a rebound of osteoclast activity in treatment groups. In this study, we chose a dose of pamidronate at, and double, the dose that preserved trabecular bone in ovariectomized rats following PTH cessation [39]. This dosing preserved the biomechanical advantage of trabecular bone in the lumbar vertebrae, and had no further effect on the sustained cortical biomechanics induced by SclAb. Therefore, these data suggest that an antiresorptive strategy involving periodic dosing may be sufficient to retain anabolic effects of SclAb gained during growth.

There are several limitations to this study. To assess bone turnover, cathepsin K imaging was performed in cessation-only animals in which all animals received SclAb. Therefore we were unable to directly monitor the antiresorptive effect of SclAb at 8 weeks compared to untreated controls using this modality, however prior results in Brtl/+ [18–20] and other OI

models [16, 17, 21], as well as pre-clinical [45, 46] and clinical osteoporosis studies [28, 47] all confirm an anti-resorptive component to SclAb therapy. MicroCT imaging was not performed in a longitudinal manner, requiring separate groups for baseline and cessation groups. However, these groups were assessed in parallel, minimizing the potential for between-cohort variation that could bias the results. We did not include a separate group of animals left untreated for the entire experiment. Continued long bone growth between 8 and 14 weeks of age may shift the trabecular region of interest slightly to include new bone not formed under the influence of SclAb. Between 8 and 14 weeks, femoral length increased 8% in Brtl/+ and 3% in WT cessation groups. These small changes represent differences in trabecular ROI length on the order of 3–7 slices, and such differences are not expected to contribute significantly to the overall results. Lastly, we cannot account for any continued cortical bone apposition or trabecular bone remodeling that may occur between 8 and 14 weeks of age due to growth alone. Of course, these results were assessed in a single mouse model of osteogenesis imperfecta with a structural type I collagen mutation in *col1a1,* and represent a single cessation time point. The restoration of phenotype following SclAb cessation likely depends on the underlying bone turnover phenotype of the animal, as well as the overall treatment effect, which is likely dependent on the type of genetic mutation and severity of disease. Furthermore, longer-term follow-up would likely require additional bouts of anti-resorptive therapy to continue to preserve anabolic gains.

In summary, following 5 weeks of SclAb therapy during a period of rapid bone growth in an OI mouse model, single administration of anti-resorptive bisphosphonate was sufficient to preserve anabolic gains at trabecular sites, but was not required to preserve cortical bone effects following 6 weeks of treatment cessation. These results are similar to clinical cessation results in post-menopausal osteoporosis, suggesting a need for sequential anabolic and anti-resorptive therapy in treatment of both growing and aged OI skeletons.

Acknowledgments

This study was supported by NIH grant AR062522. SclAb was graciously provided by Amgen and UCB. The authors thank Mike Ominsky for feedback on the data and critical review of the manuscript. The authors would like to thank Bonnie Nolan and Kathy Sweet for their technical assistance. Study designed and conducted by KMK, JEP, and MSC. Data collected by JEP, DKB, and BK. Data analyzed and interpreted by all authors. Manuscript was written and approved by all authors. KMK takes responsibility for the integrity of the data analysis.

References

1. Forlino A, Marini JC. Osteogenesis imperfecta. Lancet. 2015
2. Forlino A, Cabral WA, Barnes AM, Marini JC. New perspectives on osteogenesis imperfecta. Nat Rev Endocrinol. 2011; 7:540–57. [PubMed: 21670757]
3. Dwan K, Phillipi CA, Steiner RD, Basel D. Bisphosphonate therapy for osteogenesis imperfecta. Cochrane Database Syst Rev. 2014; 7:CD005088.
4. Hald JD, Evangelou E, Langdahl BL, Ralston SH. Bisphosphonates for the prevention of fractures in osteogenesis imperfecta: meta-analysis of placebo-controlled trials. J Bone Miner Res. 2015; 30:929–33. [PubMed: 25407702]
5. Camacho NP, Raggio CL, Doty SB, Root L, Zraick V, Ilg WA, Toledano TR, Boskey AL. A controlled study of the effects of alendronate in a growing mouse model of osteogenesis imperfecta. Calcif Tissue Int. 2001; 69:94–101. [PubMed: 11683430]

6. McCarthy EA, Raggio CL, Hossack MD, Miller EA, Jain S, Boskey AL, Camacho NP. Alendronate treatment for infants with osteogenesis imperfecta: demonstration of efficacy in a mouse model. Pediatr Res. 2002; 52:660–70. [PubMed: 12409511]
7. Misof BM, Roschger P, Baldini T, Raggio CL, Zraick V, Root L, Boskey AL, Klaushofer K, Fratzl P, Camacho NP. Differential effects of alendronate treatment on bone from growing osteogenesis imperfecta and wild-type mouse. Bone. 2005; 36:150–8. [PubMed: 15664013]
8. Uveges T, Kozloff KM, Ty JM, Ledgard F, Raggio CL, Gronowicz G, Goldstein SA, Marini JC. Alendronate treatment of Brtl osteogenesis imperfecta mouse improves femoral geometry and load response before fracture but has detrimental effects on osteoblasts and bone formation and decreases predicted material properties. Journal of Bone and Mineral Research. 2009; 24:849–859. [PubMed: 19113917]
9. Nicolaou N, Agrawal Y, Padman M, Fernandes JA, Bell MJ. Changing pattern of femoral fractures in osteogenesis imperfecta with prolonged use of bisphosphonates. J Child Orthop. 2012; 6:21–7. [PubMed: 23450103]
10. Manolopoulos KN, West A, Gittoes N. The paradox of prevention--bilateral atypical subtrochanteric fractures due to bisphosphonates in osteogenesis imperfecta. J Clin Endocrinol Metab. 2013; 98:871–2. [PubMed: 23386638]
11. Carpintero P, Del Fresno JA, Ruiz-Sanz J, Jaenal P. Atypical fracture in a child with osteogenesis imperfecta. Joint Bone Spine. 2015; 82:287–8. [PubMed: 25543273]
12. Munns CF, Rauch F, Zeitlin L, Fassier F, Glorieux FH. Delayed osteotomy but not fracture healing in pediatric osteogenesis imperfecta patients receiving pamidronate. J Bone Miner Res. 2004; 19:1779–86. [PubMed: 15476577]
13. Kamoun-Goldrat A, Ginisty D, Le Merrer M. Effects of bisphosphonates on tooth eruption in children with osteogenesis imperfecta. Eur J Oral Sci. 2008; 116:195–8. [PubMed: 18471236]
14. Gatti D, Rossini M, Viapiana O, Povino MR, Liuzza S, Fracassi E, Idolazzi L, Adami S. Teriparatide treatment in adult patients with osteogenesis imperfecta type I. Calcif Tissue Int. 2013; 93:448–52. [PubMed: 23907723]
15. Orwoll ES, Shapiro J, Veith S, Wang Y, Lapidus J, Vanek C, Reeder JL, Keaveny TM, Lee DC, Mullins MA, Nagamani SC, Lee B. Evaluation of teriparatide treatment in adults with osteogenesis imperfecta. J Clin Invest. 2014; 124:491–8. [PubMed: 24463451]
16. Jacobsen CM, Barber LA, Ayturk UM, Roberts HJ, Deal LE, Schwartz MA, Weis M, Eyre D, Zurakowski D, Robling AG, Warman ML. Targeting the LRP5 pathway improves bone properties in a mouse model of osteogenesis imperfecta. J Bone Miner Res. 2014; 29:2297–306. [PubMed: 24677211]
17. Roschger A, Roschger P, Keplingter P, Klaushofer K, Abdullah S, Kneissel M, Rauch F. Effect of sclerostin antibody treatment in a mouse model of severe osteogenesis imperfecta. Bone. 2014; 66:182–8. [PubMed: 24953712]
18. Sinder BP, Eddy MM, Ominsky MS, Caird MS, Marini JC, Kozloff KM. Sclerostin antibody improves skeletal parameters in a Brtl/+ mouse model of osteogenesis imperfecta. J Bone Miner Res. 2013; 28:73–80. [PubMed: 22836659]
19. Sinder BP, Salemi JD, Ominsky MS, Caird MS, Marini JC, Kozloff KM. Rapidly growing Brtl/+ mouse model of osteogenesis imperfecta improves bone mass and strength with sclerostin antibody treatment. Bone. 2014; 71C:115–123.
20. Sinder BP, White LE, Salemi JD, Ominsky MS, Caird MS, Marini JC, Kozloff KM. Adult Brtl/+ mouse model of osteogenesis imperfecta demonstrates anabolic response to sclerostin antibody treatment with increased bone mass and strength. Osteoporos Int. 2014; 25:2097–107. [PubMed: 24803333]
21. Grafe I, Alexander S, Yang T, Lietman C, Homan EP, Munivez E, Chen Y, Jiang MM, Bertin T, Dawson B, Asuncion F, Ke HZ, Ominsky MS, Lee B. Sclerostin antibody treatment improves the bone phenotype of Crtap mice, a model of recessive osteogenesis imperfecta. J Bone Miner Res. 2015
22. Poole KE, van Bezooijen RL, Loveridge N, Hamersma H, Papapoulos SE, Lowik CW, Reeve J. Sclerostin is a delayed secreted product of osteocytes that inhibits bone formation. FASEB J. 2005; 19:1842–4. [PubMed: 16123173]

23. Li X, Ominsky MS, Warmington KS, Morony S, Gong J, Cao J, Gao Y, Shalhoub V, Tipton B, Haldankar R, Chen Q, Winters A, Boone T, Geng Z, Niu QT, Ke HZ, Kostenuik PJ, Simonet WS, Lacey DL, Paszty C. Sclerostin antibody treatment increases bone formation, bone mass, and bone strength in a rat model of postmenopausal osteoporosis. J Bone Miner Res. 2009; 24:578–88. [PubMed: 19049336]
24. Ominsky MS, Niu QT, Li C, Li X, Ke HZ. Tissue-level mechanisms responsible for the increase in bone formation and bone volume by sclerostin antibody. J Bone Miner Res. 2014; 29:1424–30. [PubMed: 24967455]
25. Taylor S, Ominsky MS, Hu R, Pacheco E, He YD, Brown DL, Aguirre JI, Wronski TJ, Buntich S, Afshari CA, Pyrah I, Nioi P, Boyce RW. Time-dependent cellular and transcriptional changes in the osteoblast lineage associated with sclerostin antibody treatment in ovariectomized rats. Bone. 2016; 84:148–59. [PubMed: 26721737]
26. Li X, Warmington KS, Niu QT, Asuncion FJ, Barrero M, Grisanti M, Dwyer D, Stouch B, Thway TM, Stolina M, Ominsky MS, Kostenuik PJ, Simonet WS, Paszty C, Ke HZ. Inhibition of sclerostin by monoclonal antibody increases bone formation, bone mass, and bone strength in aged male rats. J Bone Miner Res. 2010; 25:2371–80.
27. Ominsky MS, Vlasseros F, Jolette J, Smith SY, Stouch B, Doellgast G, Gong J, Gao Y, Cao J, Graham K, Tipton B, Cai J, Deshpande R, Zhou L, Hale MD, Lightwood DJ, Henry AJ, Popplewell AG, Moore AR, Robinson MK, Lacey DL, Simonet WS, Paszty C. Two doses of sclerostin antibody in cynomolgus monkeys increases bone formation, bone mineral density, and bone strength. J Bone Miner Res. 2010; 25:948–959. [PubMed: 20200929]
28. McClung MR, Grauer A, Boonen S, Bolognese MA, Brown JP, Diez-Perez A, Langdahl BL, Reginster JY, Zanchetta JR, Wasserman SM, Katz L, Maddox J, Yang YC, Libanati C, Bone HG. Romosozumab in postmenopausal women with low bone mineral density. N Engl J Med. 2014; 370:412–20. [PubMed: 24382002]
29. Padhi D, Allison M, Kivitz AJ, Gutierrez MJ, Stouch B, Wang C, Jang G. Multiple doses of sclerostin antibody romosozumab in healthy men and postmenopausal women with low bone mass: a randomized, double-blind, placebo-controlled study. J Clin Pharmacol. 2014; 54:168–78. [PubMed: 24272917]
30. Padhi D, Jang G, Stouch B, Fang L, Posvar E. Single-dose, placebo-controlled, randomized study of AMG 785, a sclerostin monoclonal antibody. J Bone Miner Res. 2011; 26:19–26. [PubMed: 20593411]
31. Recker R, Benson C, Matsumoto T, Bolognese M, Robins D, Alam J, Chiang AY, Hu L, Krege JH, Sowa H, Mitlak B, Myers S. A randomized, double-blind phase 2 clinical trial of blosozumab, a sclerostin antibody, in postmenopausal women with low bone mineral density. J Bone Miner Res. 2014
32. Sinder BP, Lloyd WR, Salemi JD, Marini JC, Caird MS, Morris MD, Kozloff KM. Effect of anti-sclerostin therapy and osteogenesis imperfecta on tissue-level properties in growing and adult mice while controlling for tissue age. Bone. 2016; 84:222–229. [PubMed: 26769006]
33. Forlino A, Porter FD, Lee EJ, Westphal H, Marini JC. Use of the Cre/lox recombination system to develop a non-lethal knock-in murine model for osteogenesis imperfecta with an a1(I) G349C substitution. Variability in phenotype in BrtlIV mice. J Biol Chem. 1999; 274:37923–31. [PubMed: 10608859]
34. Kozloff KM, Carden A, Bergwitz C, Forlino A, Uveges T, Morris MD, Marini JC, Goldstein SA. Brittle IV mouse model for osteogenesis imperfecta IV demonstrates postpubertal adaptations to improve whole bone strength. J Bone Miner Res. 2004; 19:614–622. [PubMed: 15005849]
35. Uveges TE, Collin-Osdoby P, Cabral WA, Ledgard F, Goldberg L, Bergwitz C, Forlino A, Osdoby P, Gronowicz GA, Marini JC. Cellular mechanism of decreased bone in Brtl mouse model of OI: Imbalance of decreased osteoblast function and increased osteoclasts and their precursors. J Bone Miner Res. 2008; 23:1983–94. [PubMed: 18684089]
36. Black DM, Bilezikian JP, Ensrud KE, Greenspan SL, Palermo L, Hue T, Lang TF, McGowan JA, Rosen CJ. One year of alendronate after one year of parathyroid hormone (1-84) for osteoporosis. N Engl J Med. 2005; 353:555–65. [PubMed: 16093464]

37. Kurland ES, Heller SL, Diamond B, McMahon DJ, Cosman F, Bilezikian JP. The importance of bisphosphonate therapy in maintaining bone mass in men after therapy with teriparatide [human parathyroid hormone(1-34)]. Osteoporos Int. 2004; 15:992–7. [PubMed: 15175844]

38. Recknor CP, Recker RR, Benson CT, Robins DA, Chiang AY, Alam J, Hu L, Matsumoto T, Sowa H, Sloan JH, Konrad RJ, Mitlak BH, Sipos AA. The effect of discontinuing treatment with blosozumab: Follow-up results of a phase 2 randomized clinical trial in postmenopausal women with low bone mineral density. J Bone Miner Res. 2015; 30:1717–25. [PubMed: 25707611]

39. Cheng PT, Chan C, Muller K. Cyclical treatment of osteopenic ovariectomized adult rats with PTH(1-34) and pamidronate. J Bone Miner Res. 1995; 10:119–26. [PubMed: 7747618]

40. Kozloff KM, Quinti L, Patntirapong S, Hauschka PV, Tung C, Weissleder R, Mahmood U. Non-invasive optical detection of cathepsin K-mediated fluorescence reveals osteoclast activity in vitro and in vivo. Bone. 2009; 44:190–8. [PubMed: 19007918]

41. Kozloff KM, Volakis LI, Marini JC, Caird MS. Near-infrared fluorescent probe traces bisphosphonate delivery and retention in vivo. J Bone Miner Res. 2010; 25:1748–58. [PubMed: 20200982]

42. Meganck JA, Kozloff KM, Thornton MM, Broski SM, Goldstein SA. Beam hardening artifacts in micro-computed tomography scanning can be reduced by X-ray beam filtration and the resulting images can be used to accurately measure BMD. Bone. 2009; 45:1104–16. [PubMed: 19651256]

43. Otsu N. A threshold selection method from gray-level histograms. IEEE Trans Systems, Man, and Cybernetics. 1979; 91:62–66.

44. Tommasini SM, Morgan TG, van der Meulen M, Jepsen KJ. Genetic variation in structure-function relationships for the inbred mouse lumbar vertebral body. J Bone Miner Res. 2005; 20:817–27. [PubMed: 15824855]

45. Li X, Niu QT, Warmington KS, Asuncion FJ, Dwyer D, Grisanti M, Han CY, Stolina M, Eschenberg MJ, Kostenuik PJ, Simonet WS, Ominsky MS, Ke HZ. Progressive increases in bone mass and bone strength in an ovariectomized rat model of osteoporosis after 26 weeks of treatment with a sclerostin antibody. Endocrinology. 2014; 155:4785–97. [PubMed: 25259718]

46. Stolina M, Dwyer D, Niu QT, Villasenor KS, Kurimoto P, Grisanti M, Han CY, Liu M, Li X, Ominsky MS, Ke HZ, Kostenuik PJ. Temporal changes in systemic and local expression of bone turnover markers during six months of sclerostin antibody administration to ovariectomized rats. Bone. 2014; 67:305–13. [PubMed: 25093263]

47. McColm J, Hu L, Womack T, Tang CC, Chiang AY. Single- and multiple-dose randomized studies of blosozumab, a monoclonal antibody against sclerostin, in healthy postmenopausal women. J Bone Miner Res. 2014; 29:935–43. [PubMed: 23996473]

Highlights

- Sclerostin antibody induces a significant anabolic bone response in Brtl/+ mouse model for osteogenesis imperfecta.
- 6 weeks after cessation of sclerostin antibody, femoral cortical bone was resistant to cessation-induced loss of bone structure and function.
- Anabolic gains in trabecular bone were not sustained following sclerostin antibody cessation in the absence of anti-resorptive therapy.
- One-time bisphosphonate administration upon cessation was sufficient to retain trabecular bone for 6 weeks after sclerostin antibody withdrawal.

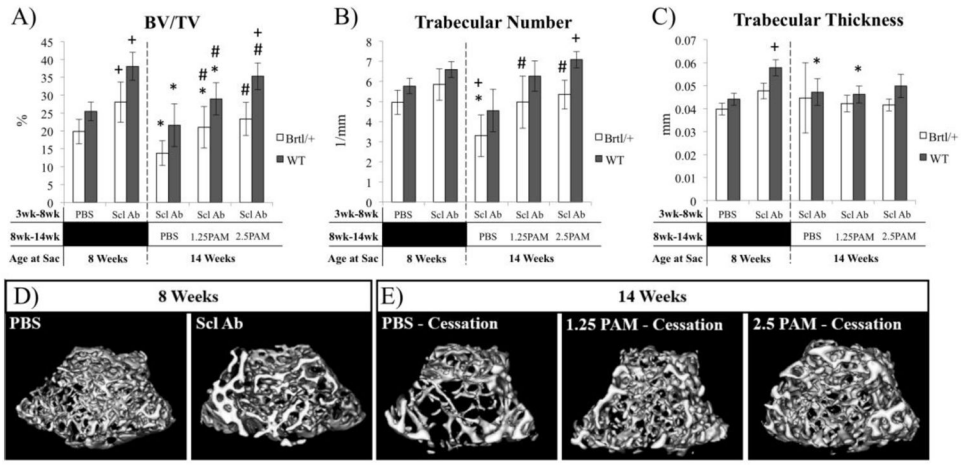

Figure 1.

MicroCT analysis of distal femoral trabecular bone following treatment (8 weeks) and cessation (14 weeks) **A)** BV/TV and **B)** Trabecular number of the distal femur show a decrease in bone mass following the cessation of SclAb treatment in both Brtl/+ and WT animals. However, when administered a single dose of PAM the anabolic gains from SclAb treatment are preserved. There is also a decrease in **C)** Trabecular thickness following treatment cessation in Brtl/+ mice and anabolic gains are preserved with a single injection of PAM. Within genotype significant differences: * vs. 8 wk SclAb; + vs. 8 wk PBS; # vs. 14 wk PBS. All symbols indicate $p < 0.05$. **D)** MicroCT isosurfaces of Brtl/+ mice administered SclAb from 3–8 weeks of age show an increase trabecular BV/TV following treatment. **E)** These gains are lost following a 6 week cessation period; however, gains are preserved when mice are given a single injection of PAM. WT mice (not shown) also show the same trend.

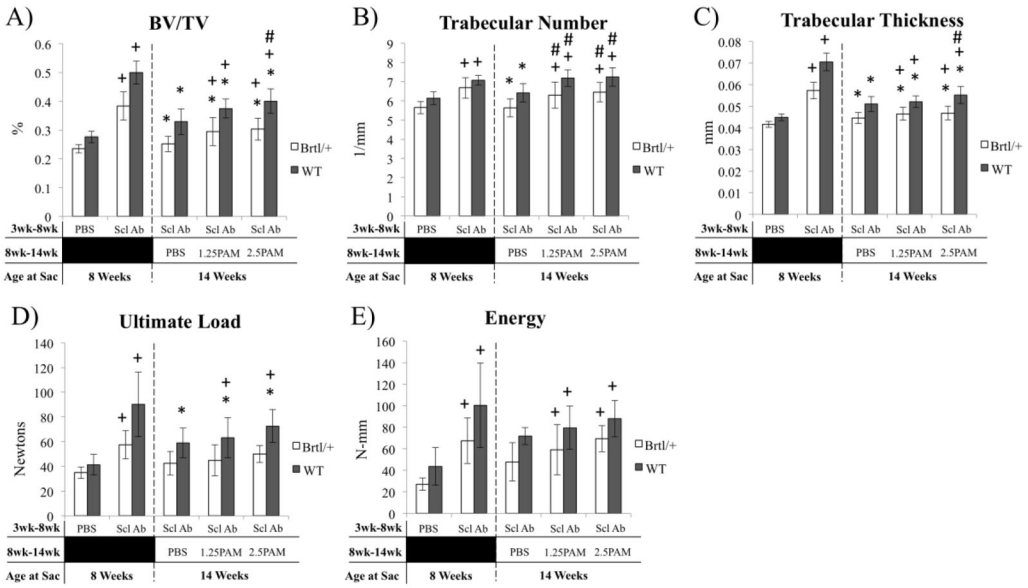

Figure 2.

MicroCT analysis (A–C) and compression testing (D–E) of the lumbar spine show similar effects to femoral anabolic and cessation outcomes. **A)** BV/TV is reduced following cessation through a reduction in both trabecular number **(B)** and thickness **(C)**. Single dose PAM preserves trabecular number dose-dependently, but trabecular thickness remains reduced during cessation. Biomechanically, Brtl/+ mice show modest, non-significant reductions in ultimate load and energy at ultimate load, while WT mice retain a treatment effect over 8 Wk PBS with PAM, despite a small reduction compared to 8 week treatment groups. Within genotype significant differences: * vs. 8 wk SclAb; + vs. 8 wk PBS; # vs. 14 wk PBS. All symbols indicate $p < 0.05$.

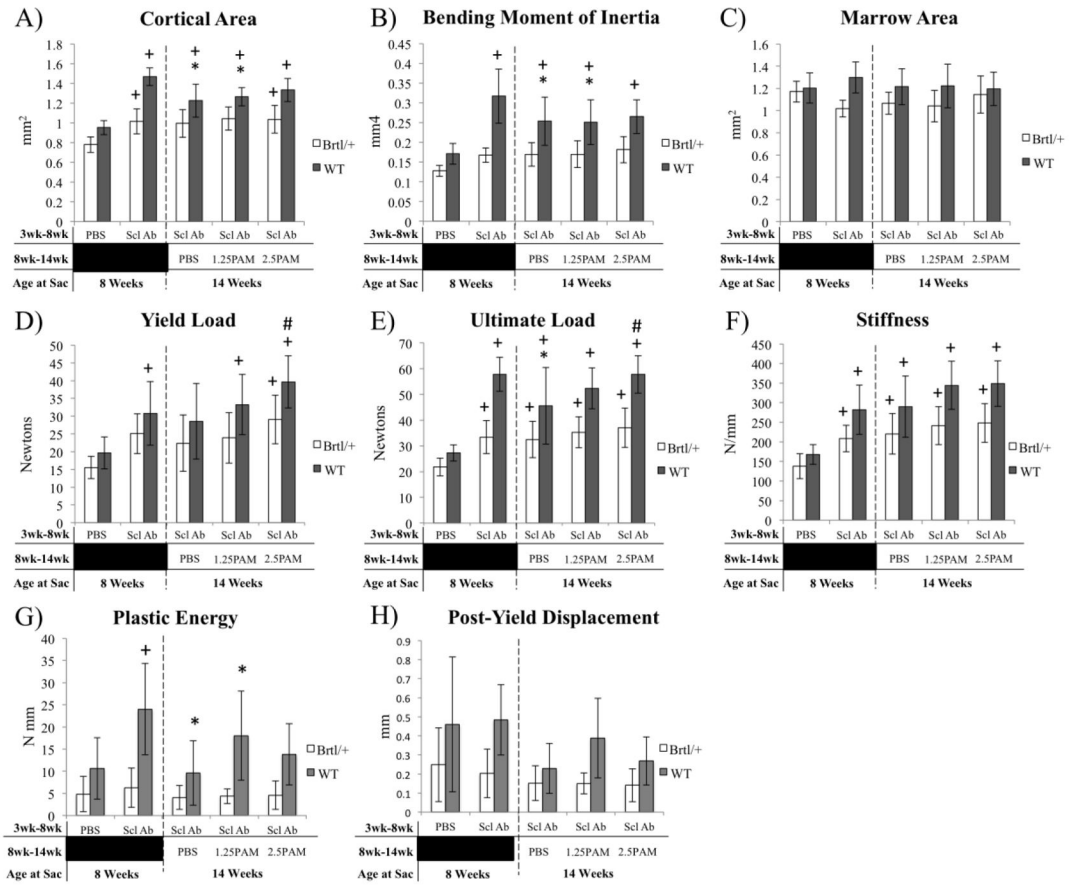

Figure 3.

MicroCT analysis (A–C) and 4-point bending (D–E) assessment of the femoral midshaft following treatment (8 weeks) and cessation (14 weeks). MicroCT reveals a preservation of bone cortical area (A), bending moment of inertia (B), and marrow area (C) in Brtl/+ without additional effects of pamidronate. Similarly, no biomechanical effects of cessation were observed in Brtl/+ yield load (D), ultimate load (E) stiffness (F), plastic energy (G) or post-yield displacement (H). WT mice showed modest decrements in cortical area and bending moment of inertia, but bone size and strength remained elevated over 8 week control mice. * vs. 8 wk SclAb; + vs. 8 wk PBS; # vs. 14 wk PBS. All symbols indicate $p < 0.05$.

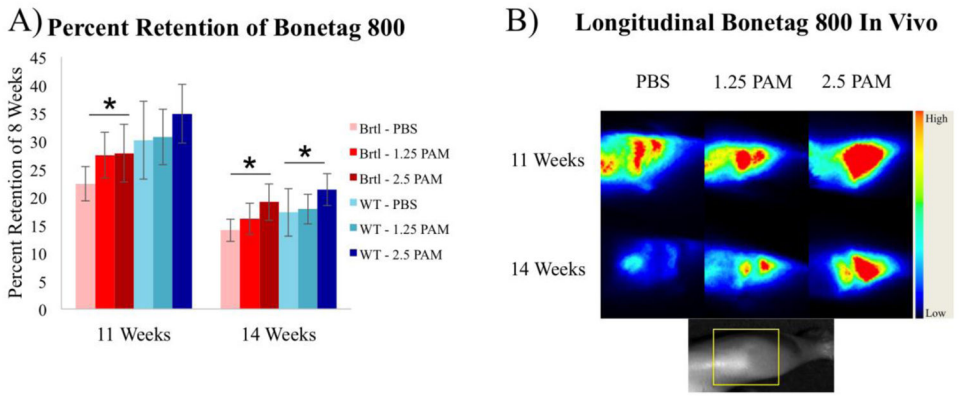

Figure 4.

Longitudinal *in vivo* imaging of proximal tibial bone loss with near-infrared tetracycline label. Bonetag 800 was administered at 8 weeks, and proximal tibial fluorescence was quantified at 8, 11, and 14 weeks and expressed as percentage of 8 week signal. A) Progressive bone loss is observed in untreated mice during SclAb cessation, which was partially prevented with increasing doses of pamidronate. B) Representative fluorescent images show probe focused at the proximal tibial growth plate is retained with increasing doses of pamidronate in mice treated with SclAb. Inset shows limb orientation with site of fluorescence encompassing distal femur/proximal tibia highlighted by yellow box. * $p<0.05$ within sample repeated measure ANOVA for Brtl/+ (red bars) and WT (blue bars).

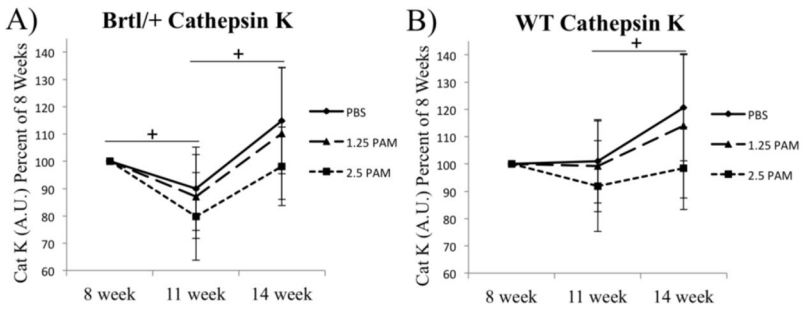

Figure 5.

Near infrared optical imaging of cathepsin K activatable substrate was visualized at 8 weeks. Subsequent imaging of probe administered at 11 and 14 weeks reveals transient reductions (11 wk) and restoration (14 wk) of osteoclast activity, particularly in Brtl/+ mice. Despite large variability, a general dose-dependent trend was noted across doses of pamidronate. + $p<0.05$ within sample repeated measure ANOVA showing effect of time following cessation.